

Electronic Supplementary Information (ESI)

**Metal promoted conversion of aromatic amines to *ortho*-phenylenediiimine
derivatives by a radical coupling path**

Debarpan Dutta,^a Suman Kundu,^a Thomas Weyhermüller^b and Prasanta Ghosh*,^a

^aDepartment of Chemistry, R. K. Mission Residential College, Narendrapur, Kolkata-103,
India

^bMax-Planck-Institut für Chemische Energiekonversion, Stiftstrasse 34-36 / D-45470
Mülheim an der Ruhr, Germany

*Correspondence to: ghosh@pghosh.in

Table of Content

Serial No.	Contents	Page No.
1.	Materials and physical measurements	S3
2.	Syntheses	S4
3.	Single crystal X-ray structure determination	S6
4.	Density functional theory (DFT) calculations	S7
5.	Crystallographic data of 1 •solvent, 2 •H ₂ O and 3 cocryst•solvent (Table S1)	S8
6.	Paramagnetic templates and isolations of 1-3 (Scheme S1)	S9
7.	Change of absorption spectra with time (Fig. S1)	S9
8.	ESI mass spectrum of (T _R) ₁ • (Fig. S2a and S2b)	S10
9.	ESI mass spectrum of (T _R) ₂ • (Fig. S3)	S11
10.	(4e+4H ⁺) oxidative intermolecular coupling between L ^{SN} H ₂ and L ₂ ^{ON} H ₂ affording 3 (Scheme S2)	S12
11.	ESI mass spectrum of (T _R) ₃ • (Fig. S4)	S13
12.	Three redox states of L ₁ ^{SNN} H ⁰ , L ₂ ^{SNN} H ⁰ and L ₃ ^{SNN} H ⁰ (Scheme S3)	S13
13.	Selected experimental and calculated bond lengths [Å] of 1 •solvent, (Table S2)	S14

14.	Molecular geometry of 2 •H ₂ O in crystals (Fig. S5)	S15
15.	Selected experimental bond lengths [Å] of 2 •H ₂ O (Table S3)	S15
16.	Molecular geometry of 3 ^{cocryst} •solvent in crystals (Fig. S6)	S16
17.	Selected experimental bond lengths [Å] of 3 ^{cocryst} •solvent (Table S4)	S16
18.	Ground electronic states of (T _R) ₁ • and (T _R) ₂ • (Scheme S4)	S17
19.	Kinetic EPR spectra of the reaction mixtures (Fig. S7)	S17-18
20.	EPR of the mixture of (T _R) ₃ • and (T _R) ₁ • in toluene (Fig. S8)	S19
21.	Cyclic voltammogram of 1 , 2 and 3 ^{cocryst} in CH ₂ Cl ₂ (Fig. S9)	S19
22.	Cyclic voltammogram data of 1 , 2 and 3 ^{cocryst} (Table S5)	S19
23.	UV-vis-NIR absorption spectra of 1 , 2 and 3 ^{cocryst} in CH ₂ Cl ₂ (Fig. S10)	S20
24.	UV-vis-NIR absorption spectral data of 1 , 2 and 3 ^{cocryst} (Table S6)	S20
25.	Frontier molecular orbitals of 1 (Fig. S11)	S21
26.	Optimized geometry and calculated UV-vis-NIR absorption spectra of 1 obtained from TD DFT calculation in CH ₂ Cl ₂ (Fig. S12)	S22
27.	Calculated significant bond lengths of (T _R) ₁ • and (T _R) ₂ • (Table S7)	S22
28.	Calculated UV-vis spectra of (T _R) ₁ • and (T _R) ₂ • in CH ₂ Cl ₂ obtained from TD DFT calculations (Fig. S13)	S23
29.	Frontier molecular orbitals of (T _R) ₁ • and (T _R) ₂ • (Fig. S14)	S24
30.	Calculated excitation energies , oscillator strengths and transition types obtained from TD DFT calculation on 1 (Table S8)	S25
31.	Gas phase and solution optimized coordinates of 1 , (T _R) ₁ • and (T _R) ₂ • (Table S9-S12)	S26-S33
32.	References	S34

Experimental section

Materials and physical measurements

Reagents or analytical grade materials were obtained from *Merck* and used without further purification. Spectroscopic grade solvents were used for spectroscopic and electrochemical measurements. The C, H and N contents of the compounds were obtained from a Perkin-Elmer 2400 Series II elemental analyzer. Infrared spectra of the samples were measured from 4000 to 400 cm⁻¹ with KBr pellets at room temperature on a Perkin-Elmer Spectrum RX 1 FT-IR spectrophotometer. ¹H NMR spectra were obtained at 295 K on a Bruker DPX 500 MHz spectrometer. ESI mass spectra were recorded on SHIMADZU LCMS-2020 mass spectrometer. Electronic absorption spectra were recorded on a Perkin-Elmer Lambda 750 spectrophotometer of range 3300-190 nm. Magnetic susceptibilities at 298 K were measured on a Sherwood Magnetic Susceptibility Balance. The X-band EPR spectra were measured on a Magnetech GmbH MiniScope MS400 spectrometer (equipped with temperature controller TC H03), where the microwave frequency was measured with an FC400 frequency counter. The EPR spectra were simulated using EasySpin 5.2 software. The electro analytical instrument, BASi Epsilon-EC for cyclic voltammetric experiments in CH₂Cl₂ solutions containing 0.2 M tetrabutylammonium hexafluorophosphate as a supporting electrolyte was used. The BASi platinum working electrode, platinum auxiliary electrode, Ag/AgCl reference electrode were used for the electrochemical measurements. The redox potential data reported were referenced to ferrocenium/ferrocene, Fc⁺/Fc, couple.

Syntheses

[Ru^{II}(L₁^{SNNH⁰})(PPh₃)Cl₂] (1•solvent). To a solution of L^{SNH₂} (41 mg, 0.20 mmol) in dry toluene (25 mL) in a round bottom flask was added [Ru^{II}(PPh₃)₃Cl₂] (95 mg, 0.10 mmol) and the mixture was stirred for 5 min. The solution turns brown. To this brown solution was added tri-ethylamine (0.75 mmol) and the mixture was stirred for 3 h in air at 298 K. A dark blue solution was obtained. It was allowed to evaporate slowly in air at room temperature. After 5-6 days, a dark-violet crystalline residue separated out, which was collected upon filtration and dried. Diffusion of *n*-hexane to a CH₂Cl₂ solution of the residue in air afforded black needles of **1•solvent**, which are collected upon filtration. Single crystals for X-ray diffraction analyses were collected from this crop. Yield: 35 mg. (42% with respect to L^{SNH₂}). Mass spectral data [electrospray ionization (ESI), positive ion, CH₂Cl₂]: *m/z* 380 for [1-2Cl]²⁺. Anal. Calcd for: C, 60.63; H, 3.99; N, 3.37. Found: C, 60.52; H, 4.05; N, 3.25. IR/cm⁻¹ (KBr): ν 3268 (m, ν_{N-H}), 2925 (m), 1629 (m), 1578 (s), 1478 (s), 1436 (m), 1092 (m), 741 (m, ν_{C-H}), 693 (m, ν_{Ru-P}), 522 (m, ν_{Ru-P}). ¹H NMR (CDCl₃, 500 MHz, 298 K): δ (ppm) 6.8 (1H, br), 7.07 (1H, t, *J* = 6.2 Hz), 7.10-7.13 (3H, m), 7.21-7.26 (6H, m), 7.28-7.32 (6H, m), 7.46-7.48 (4H, m), 7.50-7.58 (8H, m), 7.64-7.67 (3H, m), 11.26 (1H, s).

[Ru^{II}(L₂^{SNNH⁰})(PPh₃)Cl₂] (2•H₂O). To a solution of L^{SNH₂} (20 mg, 0.10 mmol) in dry toluene (25 mL) in a round bottom flask was added L₁^{ONH₂} (12 mg, 0.10 mmol) and the mixture was stirred for 5 min and the solution turned light yellow. To this solution was added [Ru^{II}(PPh₃)₃Cl₂] (95 mg, 0.10 mmol) followed by tri-ethylamine (0.75 mmol) and the mixture was stirred for 4 h in air at 298 K. Immediately, a pink solution was obtained and that turns dark purple with time. It was allowed to evaporate slowly in air at room temperature. After 6-7 days, a dark-red residue separated out, which was collected upon filtration and dried. Diffusion of *n*-hexane to a CH₂Cl₂ solution of the residue in air afforded dark purple needles

of **2**•H₂O, which are collected upon filtration. Single crystals for X-ray diffraction analysis were collected from this crop. Yield: 25 mg. (32% with respect to L₁^{ON}H₂). Mass spectral data [electrospray ionization (ESI), positive ion, CH₂Cl₂]: *m/z* 339 for [2-2Cl]²⁺. Anal. Calcd for: C, 58.89; H, 4.14; N, 3.71. Found: C, 58.75; H, 4.22; N, 3.66. IR/cm⁻¹ (KBr): ν 3305 (m, $\nu_{\text{N-H}}$), 3056 (s), 1600 (m), 1532 (m), 1480 (s), 1434 (m), 1264 (m), 1091 (m), 745 (m, $\nu_{\text{C-H}}$), 693 (m, $\nu_{\text{Ru-P}}$), 522 (m, $\nu_{\text{Ru-P}}$). ¹H NMR (CDCl₃, 500 MHz, 298 K): δ (ppm) 5.32 (1H, br), 6.01 (1H, br), 6.70 (2H, d, *J* = 8.5 Hz), 6.80-7.15 (4H, m), 7.17-7.40 (13H, m), 7.44-7.58 (3H, m), 7.58-7.66 (3H, m), 7.61 (2H, t, *J* = 11 Hz), 11.24 (1H, s), 15.34 (1H, s).

[Ru^{II}(L₃^{SNNH⁰})(PPh₃)Cl₂] (**3**•solvent). To a solution of L^{SN}H₂ (20 mg, 0.10 mmol) in dry toluene (25 mL) in a round bottom flask was added L₂^{ON}H₂ (18 mg, 0.10 mmol) and the mixture was stirred for 5 min. To this solution mixture was added [Ru^{II}(PPh₃)₃Cl₂] (95 mg, 0.10 mmol) followed by tri-ethylamine (0.75 mmol) and the mixture was stirred for 4 h in air at 298 K. A brownish solution was obtained and that turns dark green after 3 h and blue after 10 h. It was allowed to evaporate slowly in air at room temperature. After 6-7 days, a violet crystalline residue separated out, which were collected upon filtration and dried. Diffusion of *n*-hexane to a CH₂Cl₂ solution of the residue in air afforded black needles of **3**•solvent, which are collected upon filtration. Single crystals for X-ray diffraction analysis were collected from this crop. Yield: 25 mg. (30% with respect to L₂^{ON}H₂). Mass spectral data [electrospray ionization (ESI), positive ion, CH₂Cl₂]: *m/z* 371 for [3-2Cl]²⁺ and 497 for [1-2Cl-PPh₃]⁺. Anal. Calcd for: C, 61.15; H, 4.03; N, 3.40. Found: C, 61.5; H, 4.12; N, 3.25. IR/cm⁻¹ (KBr): ν 3325 (br, $\nu_{\text{N-H}}$), 3270 (m), 2924 (m, -Me), 1580 (m), 1525 (s), 1480 (m), 1435 (m), 1228 (m), 1091 (m), 741 (m, $\nu_{\text{C-H}}$), 694 (m, $\nu_{\text{Ru-P}}$), 522 (m, $\nu_{\text{Ru-P}}$).

Single crystal X-ray structure determination

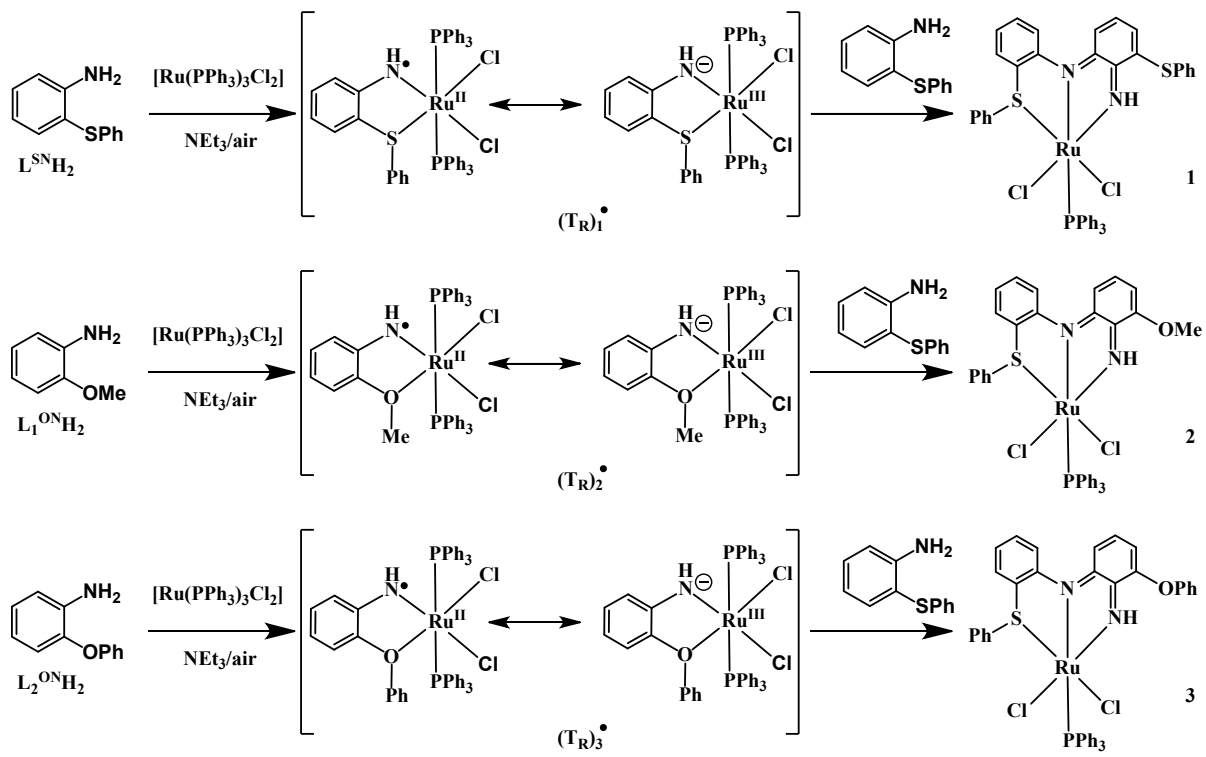
Single crystals of **1**•solvent (CCDC No. 1948967), **2**•H₂O (CCDC No. 1948968) and **3**^{cocryst}•solvent (CCDC No. 1948969) were picked up with a nylon loop and was mounted on a Bruker AXS D8 QUEST ECO diffractometer equipped with a Mo-target rotating-anode X-ray source and a graphite monochromator (Mo-K α , $\lambda = 0.71073 \text{ \AA}$). Final cell constants were obtained from least-squares fits of all measured reflections. Intensity data were corrected for absorption using intensities of redundant reflections. The structures were readily solved by direct methods and subsequent difference Fourier techniques. The crystallographic data of **1**•solvent, **2**•H₂O and **3**^{cocryst}•solvent have been listed in Table S1 (Supporting Information). The SHELXS-97 (Sheldrick 2008) software package was used for solution and SHELXL-2014/6 (Sheldrick, 2014) was used for the refinement.¹ All non-hydrogen atoms were refined anisotropically. Hydrogen atoms were placed at the calculated positions and refined as riding atoms with isotropic displacement parameters. **3**•solvent co-crystallizes with **1**•solvent and the structure of it was refined considering 70% of **3**•solvent and 30% of **1**•solvent. The probable solvent is DCM and it was removed with SQUEEZE making a void of 39 electrons, where the calculated electrons count for DCM is 42. The structure was refined applying a split atom model of the ligand fixing identical coordinates and thermal displacement parameters for N(1) and N(2) using the EXYZ and EADP instructions of SHELX.¹ The C(2)-C(6) and C(2')-C(6') carbon atoms were allowed to move and were refined using EADP, ISOR and SAME instructions. The O(1) and S(2') atoms were refined with EADP and ISOR, where distances were mildly restrained using DFIX (C-O 1.40 with delta 0.02 and C-S 1.77 with delta 0.02). The phenyl ring was treated as an ideal hexagon using AFIX 66 and ISOR.

Density functional theory (DFT) calculations

All DFT calculations were performed with the ORCA program package.² All calculations were done by the hybrid PBE0 DFT method.³ The geometry of **1** in CH₂Cl₂ (using CPCM model) was optimized with singlet and triplet spin states, while the geometries of (T_R)₁• and (T_R)₂• were optimized with doublet spin states. For all calculations, the all-electron valence double-zeta, def2-SVP,⁴ basis set with “new” polarisation function developed by Karlsruhe group was used for S, P, N, Cl, O, C and H atoms. For Ru atom def2-TZVP,⁴ a valence triple-zeta basis set with new polarisation function was used. Resolution of Identity RIJCOSX approximation^{5a} with def2/J auxiliary basis set for Coulomb and HF exchange integral for HF and hybrid DFT methods were employed for self-consistent field (SCF) gradient calculations.^{5b} The geometry optimizations were carried out in redundant internal coordinates without imposing symmetry constraints. The SCF calculations were converged tightly ($1 \times 10^{-8} E_h$ in energy, $1 \times 10^{-7} E_h$ in the density change and $1 \times 10^{-7} E_h$ in maximum element of the DIIS error vector). Time-dependent (TD) DFT^{6a-c} calculation for electronic absorption spectra was carried out on **1**, (T_R)₁• and (T_R)₂• using B3LYP functional⁷ in CH₂Cl₂ with the application of the CPCM model^{6d-e} to screen the effects of solvent.

Table S1 Crystallographic data of **1**•solvent, **2**•H₂O and **3**^{cocryst}•solvent

Complex	1 •solvent	2 •H ₂ O	3 ^{cocryst} •solvent
CCDC No	1948967	1948968	1948969
formula	C ₄₂ H ₃₃ Cl ₂ N ₂ PRuS ₂	C ₃₇ H ₃₃ Cl ₂ N ₂ O ₂ PRuS	C ₄₂ H ₃₃ Cl ₂ N ₂ O _{0.70} PRuS _{1.30}
f _w	832.76	772.65	821.52
crystal colour	black	dark red	black
crystal system	triclinic	triclinic	triclinic
space group	P-1	P-1	P-1
a/Å	9.9814(5)	10.7982(6)	9.9122(5)
b/Å	13.5654(6)	11.8469(7)	13.5323(7)
c/Å	15.3462(7)	14.5710(8)	15.4334(7)
α/°	102.105(2)	83.920(3)	102.528(2)
β/°	95.801(2)	83.224(3)	94.871(2)
γ/°	101.584(2)	68.376(3)	101.684(2)
V/Å ³	1967.95(16)	1716.77(17)	1960.94(17)
Z	2	2	2
T/K	293(2)	293(2)	293(2)
ρ calcd (g cm ⁻³)	1.405	1.495	1.391
refl. Collected (2θ _{max})	56.72	54.99	51.51
unique refl.	31467	12621	20135
ref (I>2σ)	8642	5546	6233
λ(Å)	0.71073	0.71073	0.71073
μ(mm ⁻¹)	0.713	0.756	0.680
F(000)	848	788	837
R ₁ ^a [I>2σ(I)]	0.0380	0.0601	0.0775
GOF ^b	1.114	1.087	1.137
R ₁ ^a (all data)	0.0453	0.0974	0.0904
wR ₂ ^c [I>2σ(I)]	0.0893	0.1218	0.1964
no. of Parameter/restr.	452/0	422/47	468/107
residual density (eÅ ⁻³)	0.733/-0.796	1.408/-1.173	1.668/-1.123
Observation criterion: I > 2σ(I). ^a R ₁ = Σ F _o - F _c / ΣF _o ^b GOF = {Σ[w(F _o ² - F _c ²) ²] / (n-p)} ^{1/2}			
W ^c R ₂ = {Σ[w(F _o ² - F _c ²) ²] / Σ[w(F _o ²) ²]} ^{1/2} where w = 1/[σ ² (F _o ²) + (aP) ² +bP], P = (F _o ² +2F _c ²)/3			



Scheme S1 Paramagnetic templates and isolations of **1-3**.

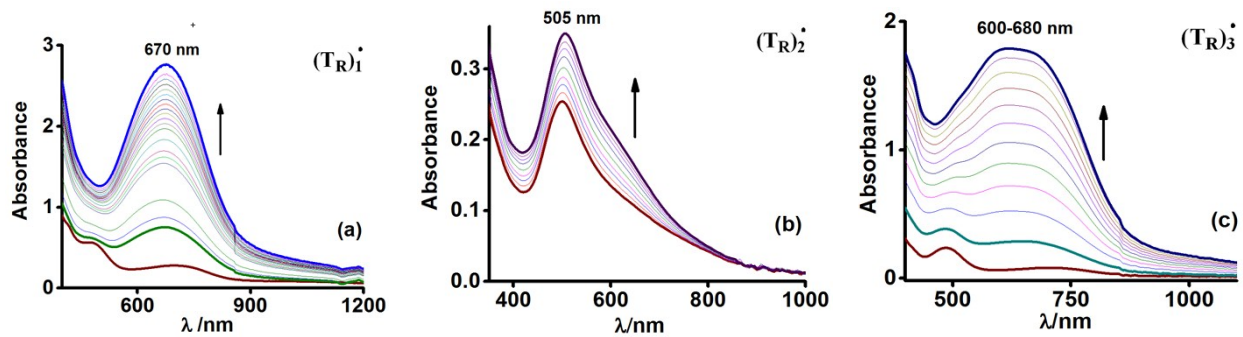


Fig. S1 Change of absorption spectra with time at the interval of 3 min for the reactions of $[\text{Ru}^{\text{II}}(\text{PPh}_3)_3\text{Cl}_2]$ with (a) $\text{L}^{\text{SN}}\text{H}_2$, (b) $\text{L}^{\text{SN}}\text{H}_2 + \text{L}_1^{\text{ON}}\text{H}_2$ (1:1) and (c) $\text{L}^{\text{SN}}\text{H}_2 + \text{L}_2^{\text{ON}}\text{H}_2$ (1:1) in dry toluene at 298 K.

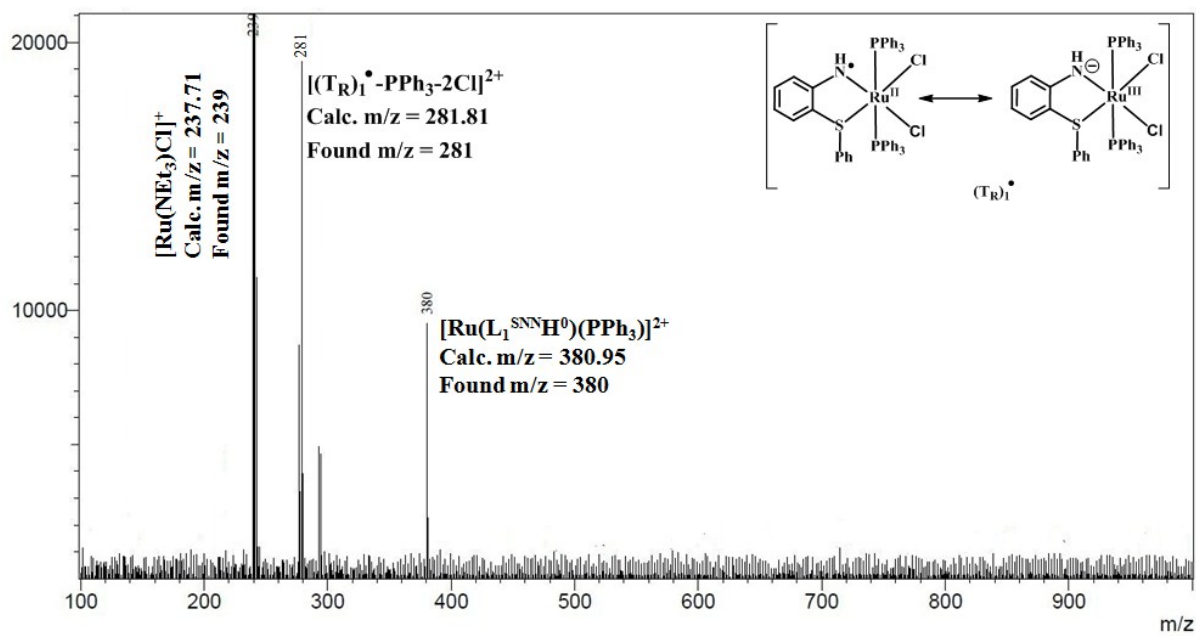


Fig. S2a ESI mass spectrum of $(T_R)_1^{\bullet}$ in green solution during $2L_1^{SNH_2} \rightarrow L_1^{SNNH^0}$ conversion.

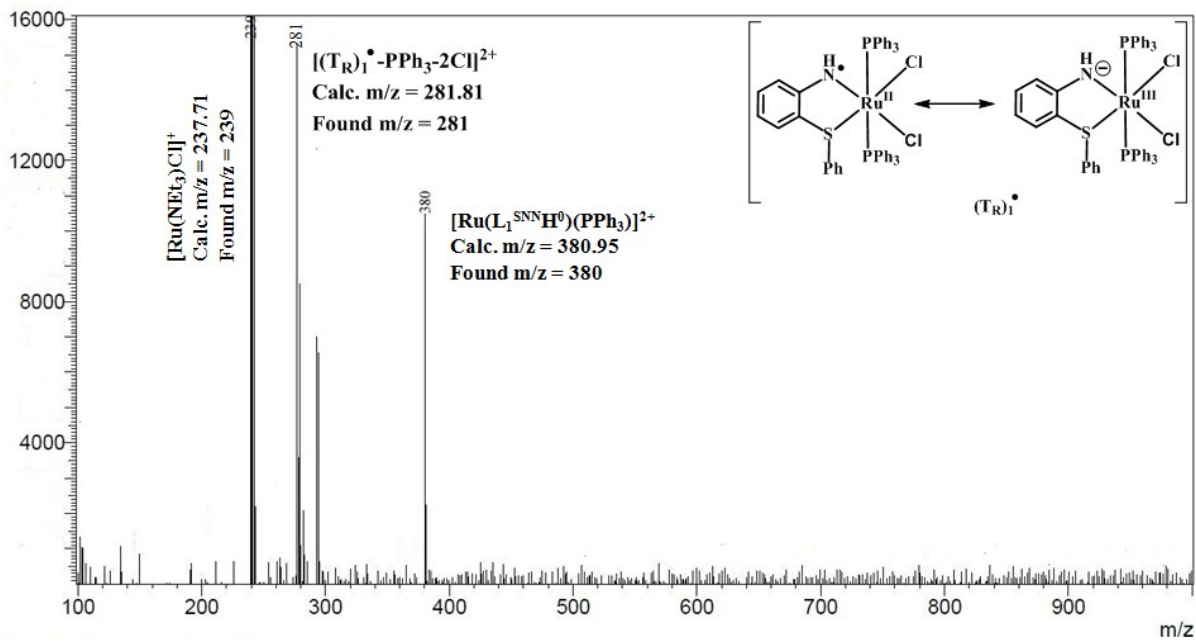


Fig. S2b ESI mass spectrum of $(T_R)_1^{\bullet}$ in blue solution during $2L_1^{SNH_2} \rightarrow L_1^{SNNH^0}$ conversion.

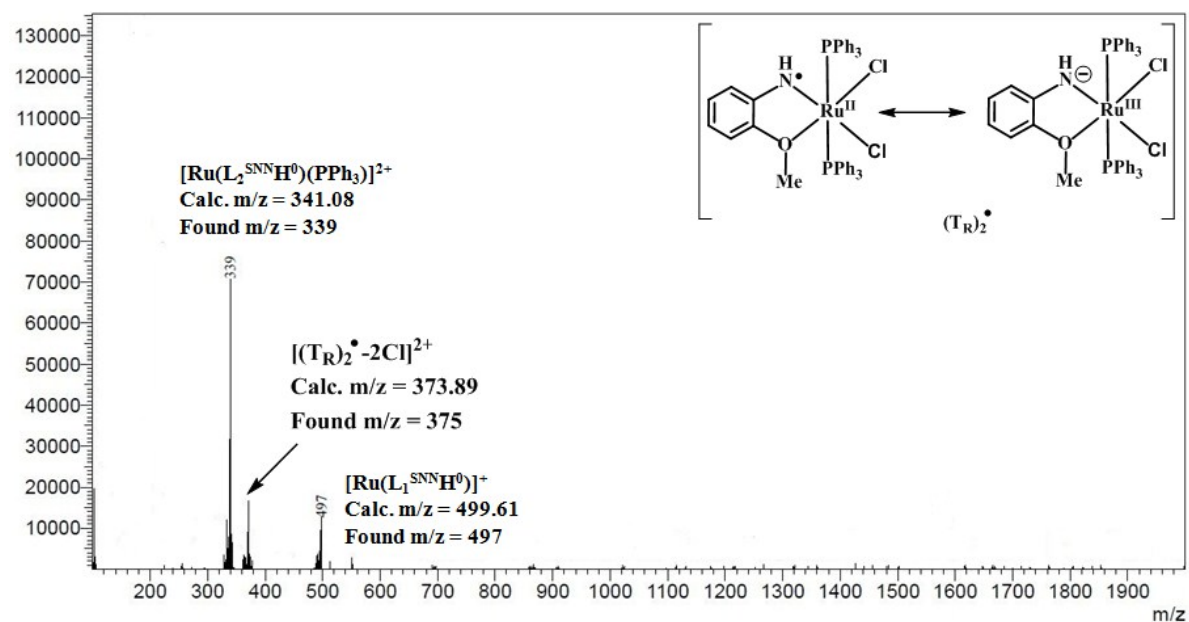
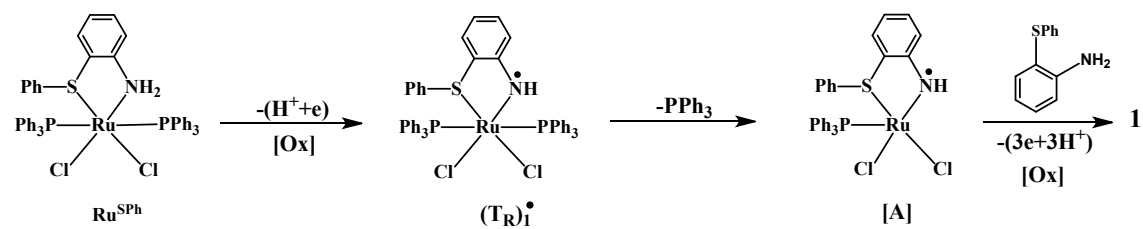
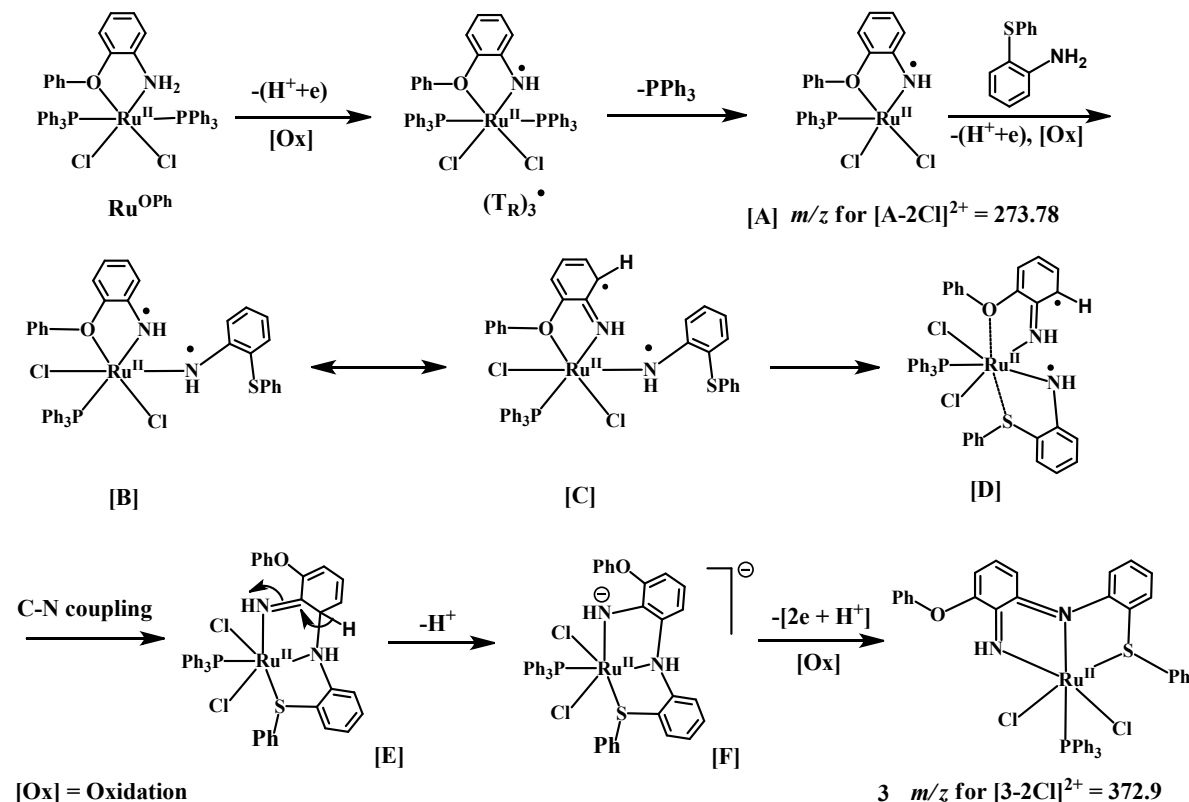


Fig. S3 ESI mass spectrum of $(T_R)_2^\bullet$ during $(L^{SN}H_2 + L_1^{ON}H_2) \rightarrow L_2^{SNN}H^0$ conversion.

Path 1:



Path 2:



$[\text{Ox}] = \text{Oxidation}$

Scheme S2 ($4\text{e} + 4\text{H}^+$) oxidative intermolecular coupling between L^{SNH_2} and $\text{L}_2^{\text{ONH}_2}$ affording **3**.

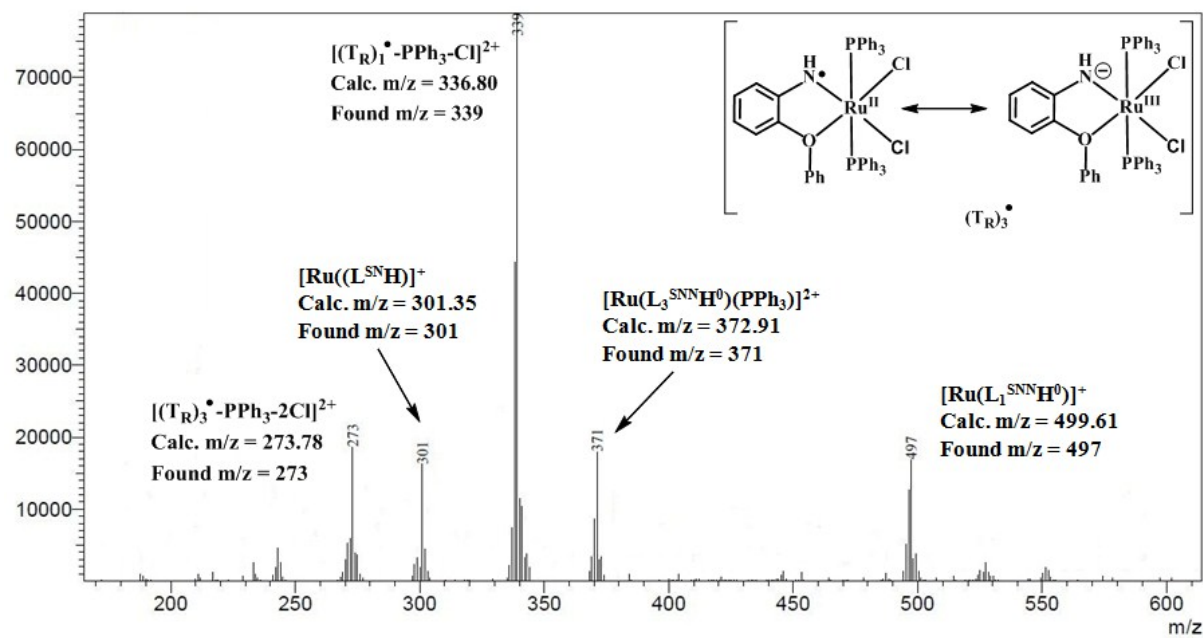
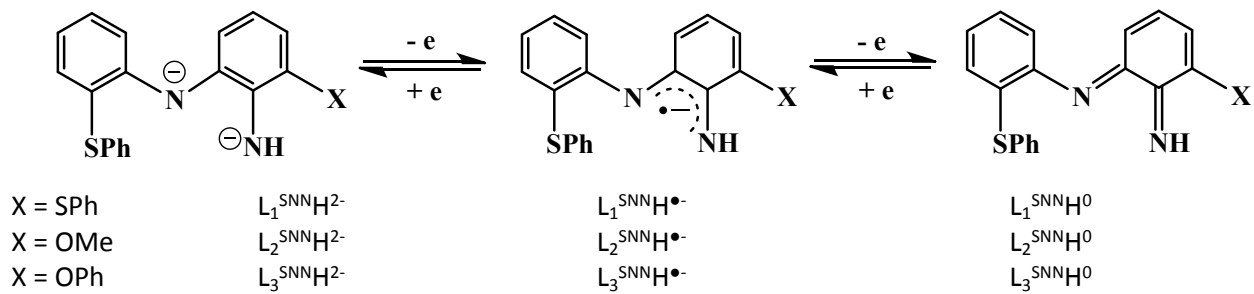


Fig. S4 ESI mass spectrum of $(T_R)_3^{\bullet}$ during $(L^{SN}H_2 + L_2^{ON}H_2) \rightarrow L_3^{SNN}H^0$ conversion.



Scheme S3 Three redox states of $L_1^{SNN}H^0$, $L_2^{SNN}H^0$ and $L_3^{SNN}H^0$.

Table S2 Selected experimental bond lengths [Å] of **1**•solvent, and the corresponding calculated bond lengths of **1** with singlet and triplet states

	Experimental	Calculated 1 ($S = 0$)	Calculated 1 ($S = 1$)
Ru(1)-N(1)	1.982(2)	1.964	1.959
Ru(1)-N(2)	1.973(2)	1.968	1.975
Ru(1)-S(1)	2.369 (1)	2.388	2.395
Ru(1)-Cl(1)	2.410(1)	2.419	2.397
Ru(1)-Cl(2)	2.424(1)	2.412	2.391
Ru(1)-P(1)	2.321(1)	2.339	2.415
C(1)-N(1)	1.315(3)	1.321	1.346
C(6)-N(2)	1.355(3)	1.347	1.382
C(1)-C(2)	1.436(4)	1.433	1.418
C(2)-C(3)	1.363(5)	1.374	1.391
C(3)-C(4)	1.423(5)	1.423	1.400
C(4)-C(5)	1.359(4)	1.373	1.393
C(5)-C(6)	1.422(4)	1.422	1.402
C(6)-C(1)	1.450(4)	1.453	1.439
C(7)-N(2)	1.416(3)	1.398	1.388
C(12)-S(1)	1.777(3)	1.782	1.782
C(7)-C(12)	1.409(4)	1.411	1.418
C(2)-S(2)	1.774(3)	1.768	1.769
C(7)-C(8)	1.398(4)	1.407	1.411
C(8)-C(9)	1.383(4)	1.389	1.389
C(9)-C(10)	1.375(5)	1.396	1.397
C(10)-C(11)	1.389(5)	1.392	1.391
C(11)-C(12)	1.390(4)	1.394	1.395

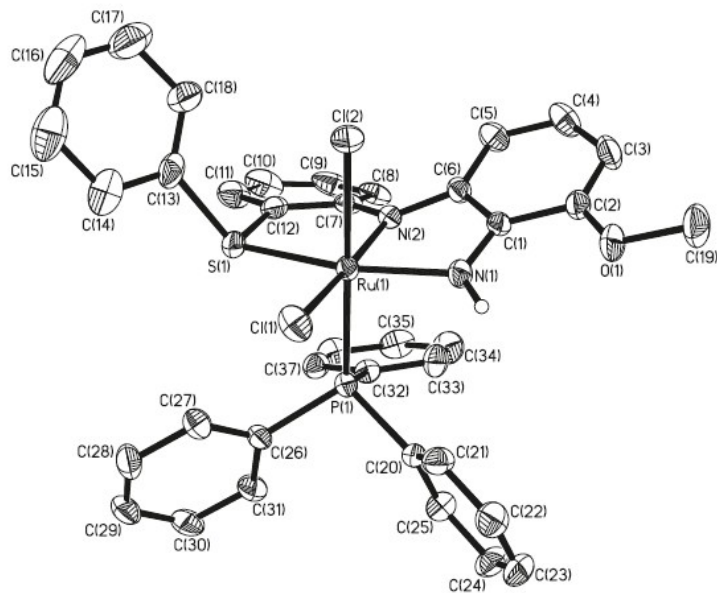


Fig. S5 Molecular geometries of **2•H₂O** in crystals (50% thermal ellipsoids, solvent molecules and hydrogen atoms are omitted for clarity).

Table S3 Selected experimental bond lengths [Å] of **2•H₂O**

Ru(1)-N(1)	2.009(4)	C(1)-C(2)	1.437(6)
Ru(1)-N(2)	1.981(4)	C(2)-C(3)	1.361(8)
Ru(1)-S(1)	2.362(2)	C(3)-C(4)	1.414(9)
Ru(1)-Cl(1)	2.431(2)	C(4)-C(5)	1.361(8)
Ru(1)-Cl(2)	2.438(2)	C(5)-C(6)	1.411(7)
Ru(1)-P(1)	2.333(2)	C(6)-C(1)	1.447(7)
C(1)-N(1)	1.314(6)	C(7)-C(12)	1.406(7)
C(6)-N(2)	1.371(6)	C(2)-O(1)	1.345(7)
C(7)-N(2)	1.390(6)	C(19)-O(1)	1.440(6)
C(12)-S(1)	1.780(6)	C(13)-S(1)	1.803(6)

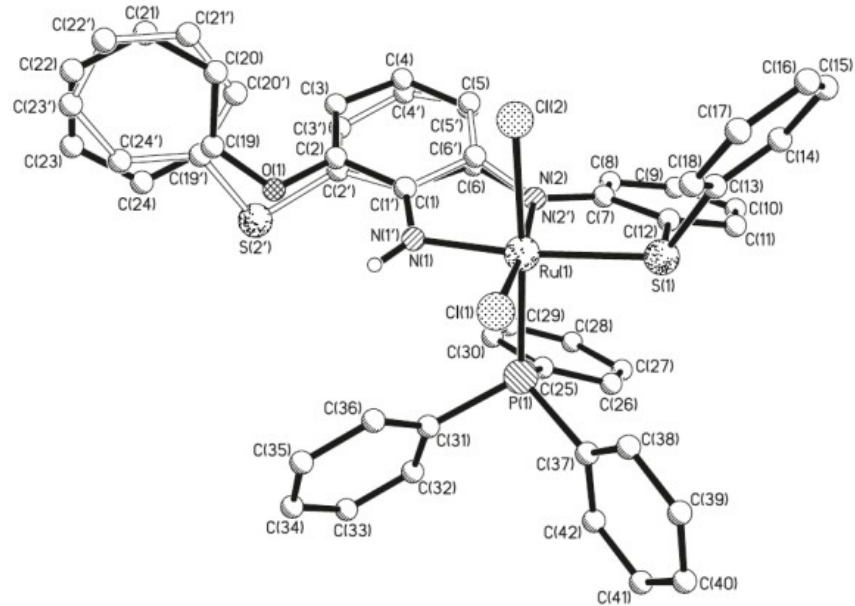
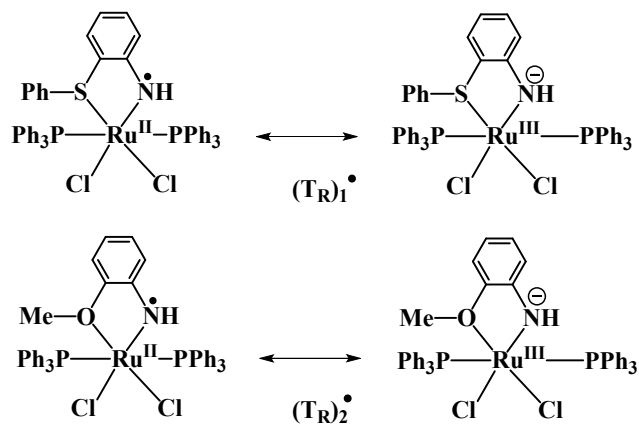


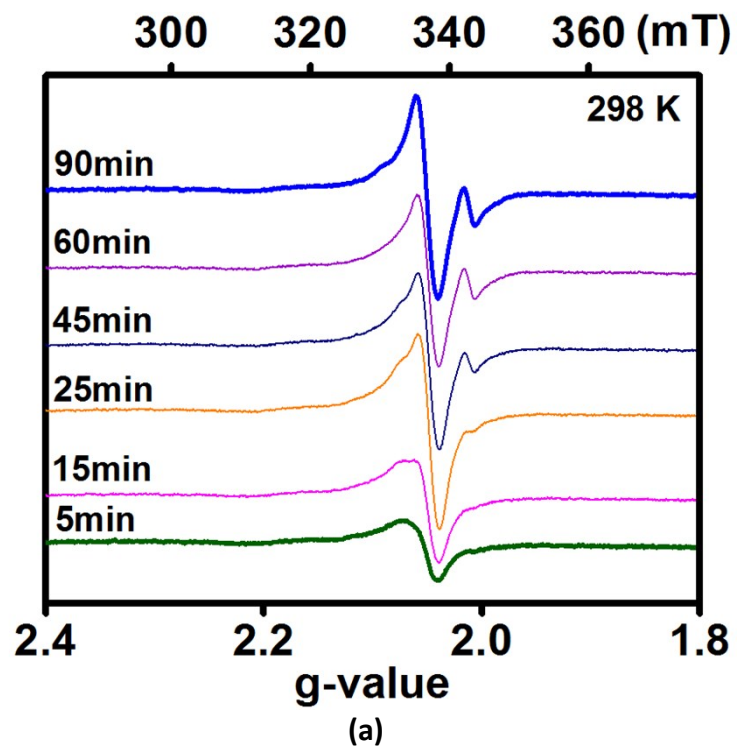
Fig. S6 Molecular geometry of **3**^{cocryst}•solvent in crystals showing the orientations of the $L_1^{SNNH^0}$ and $L_3^{SNNH^0}$ ligands (40% ellipsoid and solvent was removed by SQUEEZE).

Table S4 Selected experimental bond lengths [\AA] of **3**^{cocryst}•solvent

Ru(1)-N(1)	1.971(7)	Ru(1)-N(1')	1.971(7)
Ru(1)-N(2)	1.973(6)	Ru(1)-N(2')	1.973(6)
Ru(1)-Cl(1)	2.414(2)	Ru(1)-Cl(2)	2.431(2)
Ru(1)-S(1)	2.366 (2)	Ru(1)-P(1)	2.313(2)
C(1)-N(1)	1.309(11)	C(1')-N(1')	1.310(13)
C(6)-N(2)	1.348(10)	C(6')-N(2')	1.351(13)
C(1)-C(2)	1.434(15)	C(1')-C(2')	1.433(17)
C(2)-C(3)	1.341(16)	C(2')-C(3')	1.342(18)
C(3)-C(4)	1.410(16)	C(3')-C(4')	1.411(18)
C(4)-C(5)	1.370(2)	C(4')-C(5')	1.370(2)
C(5)-C(6)	1.420(12)	C(5')-C(6')	1.421(13)
C(6)-C(1)	1.456(13)	C(6')-C(1')	1.458(15)
C(2)-O(1)	1.367(14)	C(2')-S(2')	1.765(18)
C(19)-O(1)	1.366(13)	C(19')-S(2')	1.731(17)
C(7)-N(2)	1.422(9)	C(7)-N(2')	1.422(9)
C(7)-C(12)	1.413(11)	C(12)-S(1)	1.776(8)
C(13)-S(1)	1.793(8)		



Scheme S4 Ground electronic states of $(T_R)_1^\bullet$ and $(T_R)_2^\bullet$.



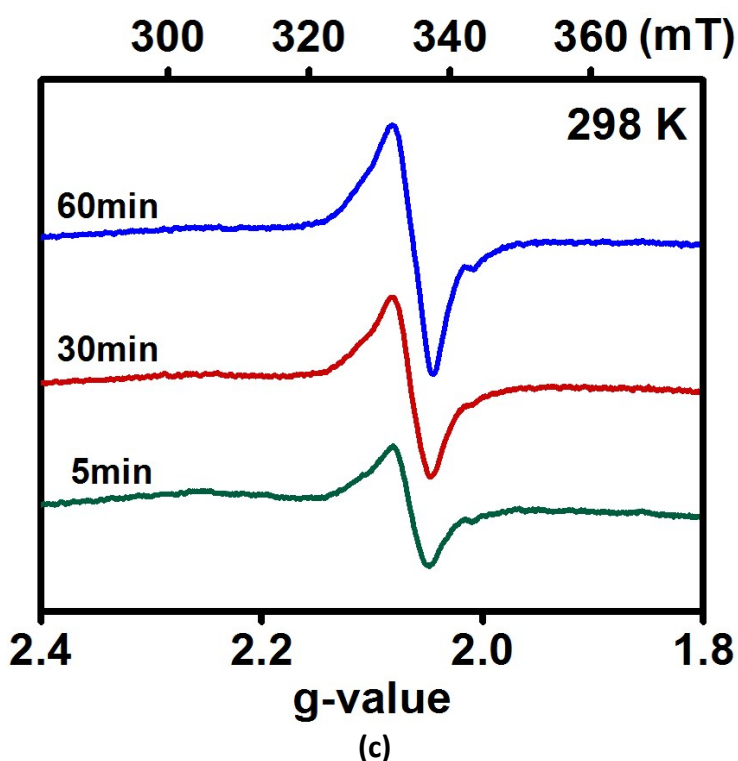
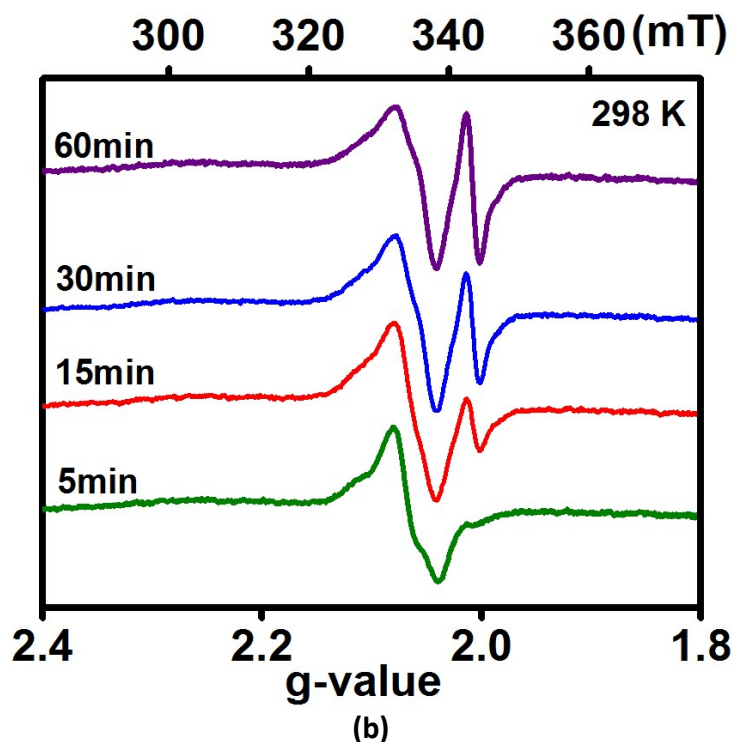


Fig. S7 Kinetic EPR spectra of the reaction mixtures of (a) LSNH_2 and Ru^{P} , (b) $\text{LSN}\text{H}_2 + \text{L}_1\text{ON}\text{H}_2$ (1:1) and Ru^{P} and (c) $\text{LSN}\text{H}_2 + \text{L}_2\text{ON}\text{H}_2$ (1:1) and Ru^{P} in dry toluene in presence of tri-ethylamine at 298 K.

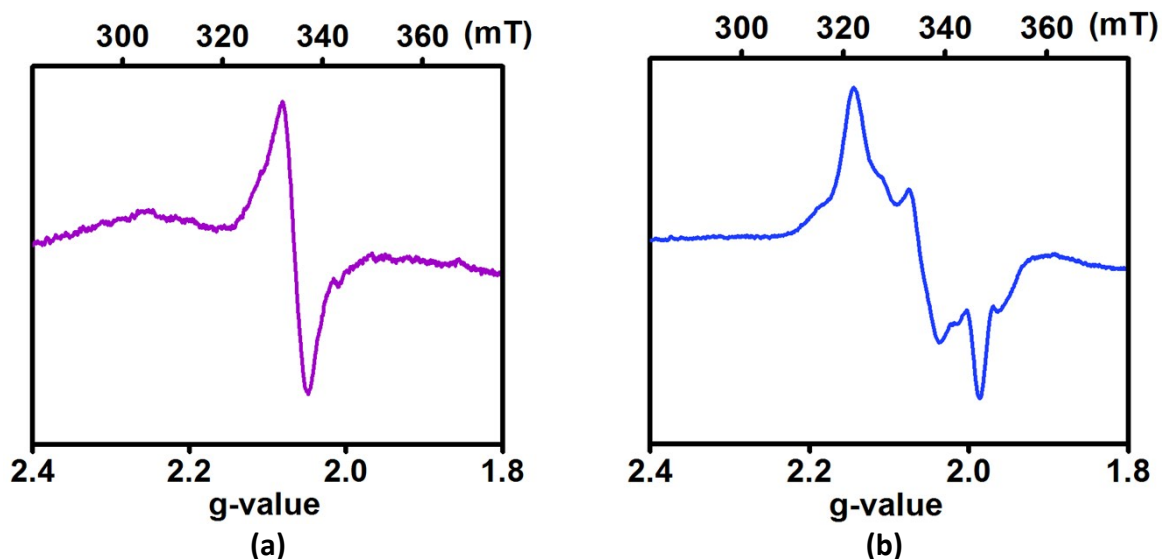


Fig. S8 (a) Fluid solution (298 K) and (b) frozen glass (113 K) EPR of the mixture of $(T_R)_3^\bullet$ and $(T_R)_1^\bullet$ in toluene.

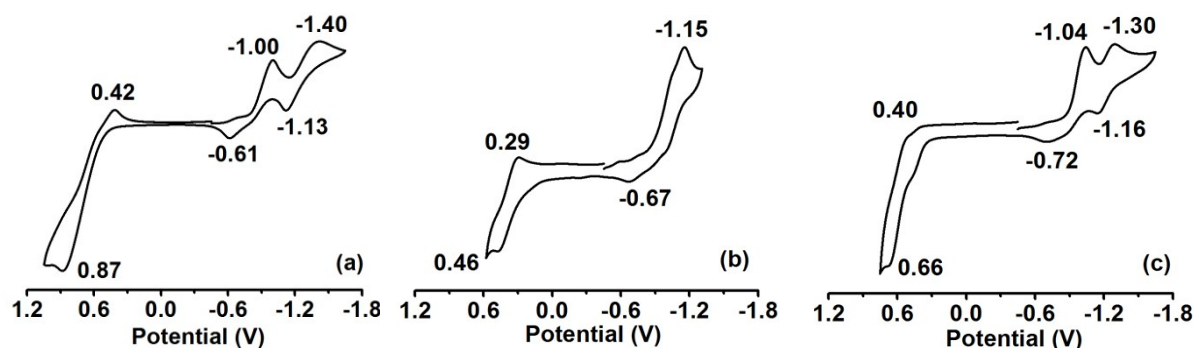


Fig. S9 Cyclic voltammogram of **1**, **2** and **3**^{cocryt} in CH_2Cl_2 containing 0.2 M $[\text{N}(n\text{-Bu})_4]\text{PF}_6$ as a supporting electrolyte at 298 K (potential is referenced to Fc^+/Fc couple).

Table S5 Cyclic voltammogram data of **1**, **2** and **3**^{cocryt} in CH_2Cl_2 containing 0.2 M $[\text{N}(n\text{-Bu})_4]\text{PF}_6$ as a supporting electrolyte at 298 K (potential is referenced to Fc^+/Fc couple)

Complexes	$E_{1/2}$ (V) (ΔE^c , mV)	$E_{1/2}$ (V) (ΔE^c , mV)
1	0.64 (450)	-0.80 (390), -1.26 (270)
2	0.37 (170)	-0.91 (480)
3 ^{cocryt}	0.53 (260)	-0.88 (320), -1.23 (140)

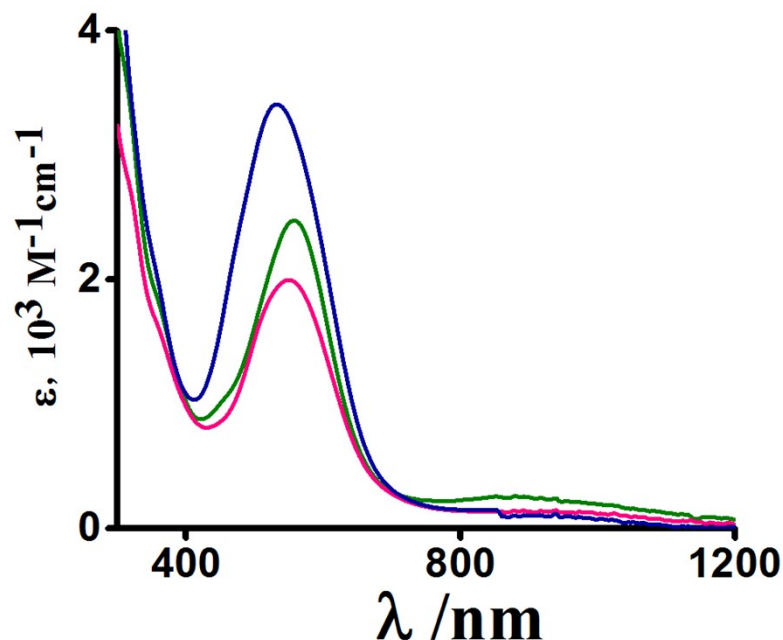


Fig. S10 UV-vis-NIR absorption spectra of **1** (olive), **2** (blue) and **3**^{cocryst} (red) in CH_2Cl_2 at 298 K.

Table S6 UV-vis-NIR absorption spectral data of **1**, **2** and **3**^{cocryst} in CH_2Cl_2 at 298 K

Compounds	λ_{\max} , nm (ϵ , $10^3 \text{ M}^{-1}\text{cm}^{-1}$)
1	950 (0.21), 560 (2.47)
2	920 (0.08), 535 (3.41)
3 ^{cocryst}	970 (0.14), 550 (2.00)

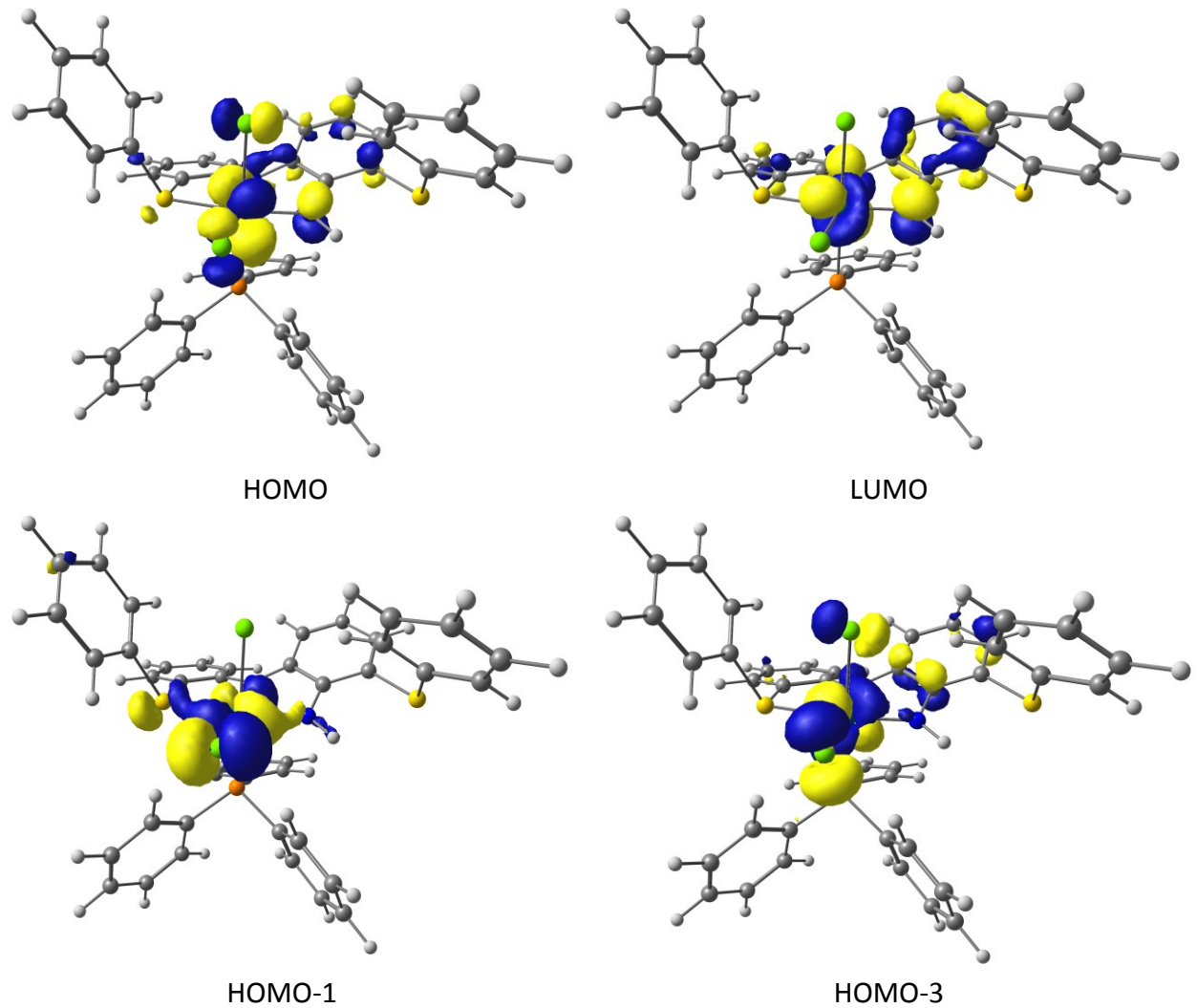
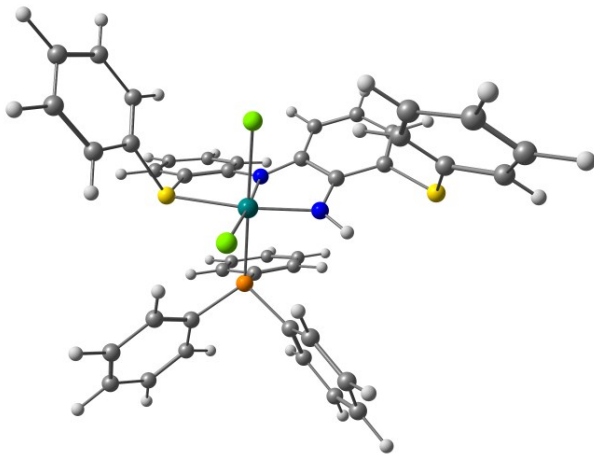
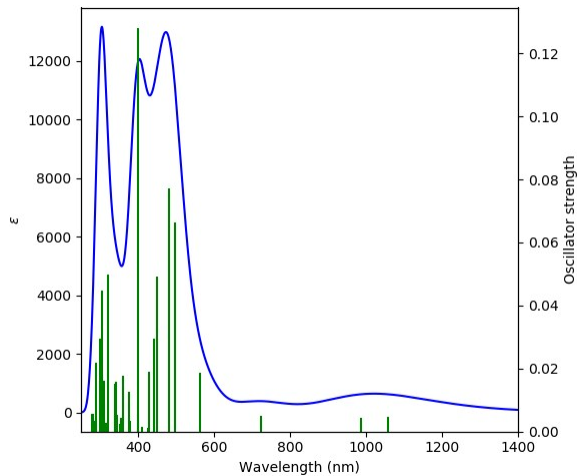


Fig. S11 Frontier molecular orbitals of **1**.



(a)



(b)

Fig. S12 (a) Optimized geometry of **1** in CH_2Cl_2 using singlet spin state and (b) Calculated UV-vis-NIR absorption spectra of **1** obtained from TD DFT calculation in CH_2Cl_2 using B3LYP functional.

Table S7 Calculated significant bond lengths [\AA] of $(\text{T}_R)_1^\bullet$ and $(\text{T}_R)_2^\bullet$

	$(\text{T}_R)_1^\bullet$	$(\text{T}_R)_2^\bullet$
Ru(1)-P(1)	2.481	2.399
Ru(1)-P(2)	2.425	2.411
Ru(1)-Cl(1)	2.430	2.423
Ru(1)-Cl(2)	2.407	2.374
Ru(1)-N(1)	1.939	1.929
Ru(1)-X(1)	1.349	1.186
C(1)-X(1)	1.781	1.368
C(1)-N(2)	1.363	1.365
C(1)-C(2)	1.419	1.420
C(2)-C(3)	1.412	1.407
C(3)-C(4)	1.387	1.392
C(4)-C(5)	1.399	1.394
C(5)-C(6)	1.396	1.399
C(6)-C(1)	1.391	1.386

$(\text{T}_R)_1^\bullet \quad X = \text{S}, R = \text{Ph}$
 $(\text{T}_R)_2^\bullet \quad X = \text{O}, R = \text{Me}$

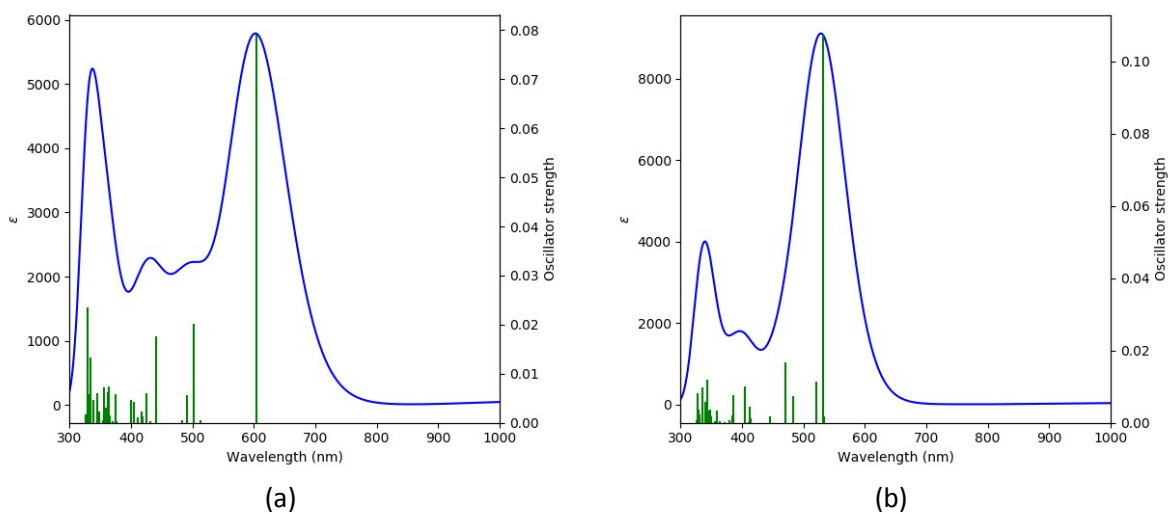
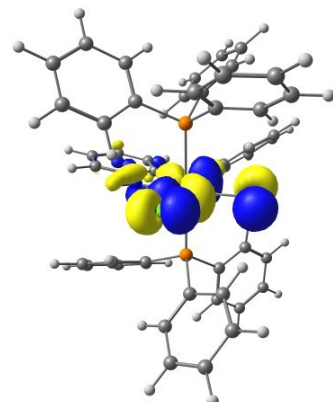
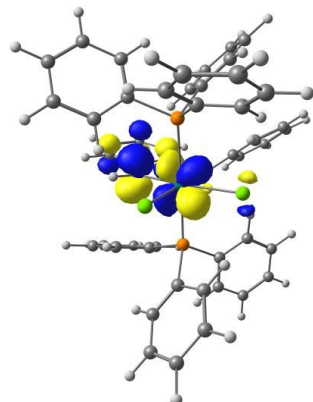


Fig. S13 Calculated UV-vis spectra of (a) $(T_R)_1^\bullet$ and (b) $(T_R)_2^\bullet$ in CH_2Cl_2 obtained from TD DFT calculations using hybrid B3LYP functional.

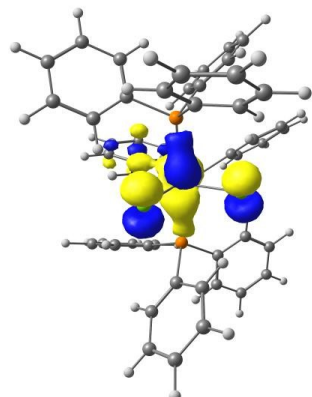
$(T_R)_1^\bullet$



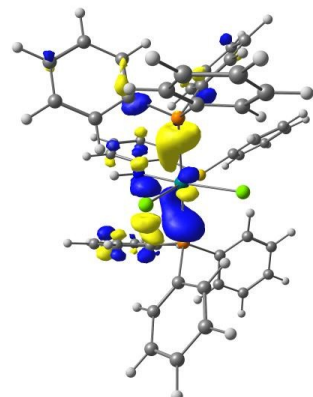
$\beta\text{-HOMO}$



$\beta\text{-LUMO}$

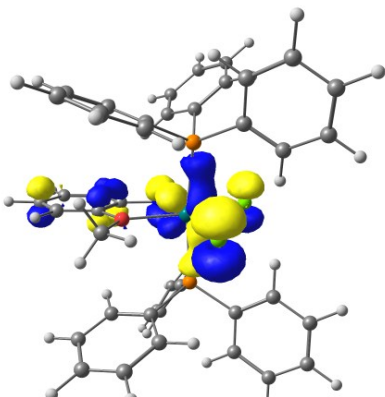


$\beta\text{-HOMO-2}$

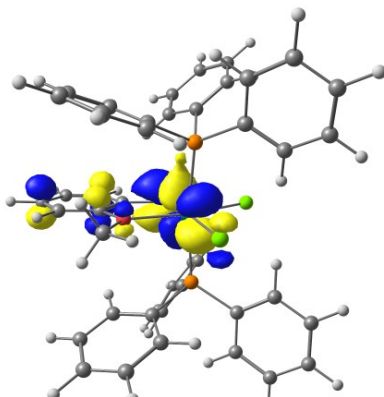


$\beta\text{-HOMO-3}$

$(T_R)_2^\bullet$



$\beta\text{-HOMO-2}$



$\beta\text{-LUMO}$

Fig. S14 Frontier molecular orbitals of $(T_R)_1^\bullet$ and $(T_R)_2^\bullet$.

Table S8 Calculated excitation energies (λ/nm), oscillator strengths (f) and transition typesobtained from TD DFT calculation on **1** in CH_2Cl_2 using PBE0 hybrid functional

λ_{cal}	f	λ_{exp}	Significant Transitions (>10%)	Transitions Types
1				
1056.9	0.005	950	HOMO → LUMO (61%) HOMO-1 → LUMO (29%)	mixed-metal-ligand to mixed-metal-ligand charge transfer transition
988.0	0.004		HOMO-1 → LUMO (60%) HOMO → LUMO (25%)	mixed-metal-ligand to mixed-metal-ligand charge transfer transition
495.9	0.066	560	HOMO-3 → LUMO (47%)	metal to mixed-metal-ligand charge transfer transitions.
480.0	0.077		HOMO-5 → LUMO (57%) HOMO-6 → LUMO (16%)	metal to mixed-metal-ligand charge transfer transitions.
$(T_R)_1^\bullet$				
603.6	0.08	670	β -HOMO-2 → LUMO (78%)	mixed-metal-ligand to mixed-metal-ligand charge transfer transition
501.2	0.02		β -HOMO-3 → LUMO (92%)	mixed-metal-ligand to mixed-metal-ligand charge transfer transition
$(T_R)_2^\bullet$				
532.3	0.107	505	β -HOMO-2 → LUMO (83%)	mixed-metal-ligand to mixed-metal-ligand charge transfer transition

Table S9 Optimized coordinates of **1** in CH₂Cl₂ with singlet spin state

Ru	5.292416	1.032105	10.173972
P	4.363996	1.933579	12.122590
S	4.288422	2.771249	8.880918
Cl	7.357125	2.237372	10.542938
Cl	6.358849	0.124734	8.209579
S	6.604167	-3.486484	12.038767
N	5.679648	-0.649948	11.111329
H	6.325295	-0.860585	11.876970
N	3.753057	-0.033599	9.600526
C	5.168742	1.463497	13.714320
C	5.059588	-1.691006	10.585364
C	3.979408	-1.359769	9.671045
C	4.998952	3.026503	7.254757
C	4.240893	3.757628	12.337502
C	2.647803	1.310397	12.295493
C	3.322734	-2.410988	8.973254
H	2.585061	-2.182670	8.205152
C	5.136329	4.600070	11.667568
H	5.871231	4.167121	10.984155
C	2.641595	0.565149	8.999387
C	4.540852	2.378966	6.107846
H	3.753916	1.625152	6.174053
C	4.425422	1.378736	14.901124
H	3.337673	1.480314	14.880091
C	2.773481	1.894929	8.546318
C	6.561570	1.321819	13.768982
H	7.150130	1.410630	12.851081
C	3.339202	4.309350	13.262145
H	2.643174	3.669451	13.808821
C	5.371706	-3.066212	10.842132
C	1.710346	2.556800	7.933042
H	1.846107	3.583203	7.584061
C	3.666064	-3.715386	9.230896
H	3.178287	-4.519640	8.676940
C	6.027435	3.969844	7.180366
H	6.393327	4.462236	8.083943
C	2.445720	-0.004913	12.739518
H	3.295549	-0.615954	13.053926
C	5.123897	5.974281	11.914763
H	5.832428	6.622383	11.393648
C	8.167769	-3.150771	11.242220
C	1.544647	2.060943	11.871585
H	1.680989	3.076255	11.492964
C	1.381639	-0.049527	8.880560
H	1.212205	-1.034062	9.315179
C	0.328086	0.611662	8.261052
H	-0.639689	0.111722	8.177421
C	6.454466	1.039982	16.171334
H	6.958839	0.878158	17.127336

C	7.196947	1.109015	14.993732
H	8.284190	0.999709	15.024928
C	4.674377	-4.046599	10.178816
H	4.931432	-5.093518	10.356599
C	5.093396	2.709974	4.870772
H	4.722704	2.210417	3.972090
C	3.325139	5.682334	13.500140
H	2.617419	6.101777	14.219742
C	4.218781	6.516661	12.826215
H	4.215540	7.592004	13.024276
C	6.584139	4.280558	5.940683
H	7.386702	5.019982	5.879342
C	0.490710	1.907480	7.766083
H	-0.338870	2.421259	7.276135
C	6.109309	3.663069	4.782469
H	6.536381	3.927452	3.811937
C	9.290112	-3.715896	11.862948
H	9.162760	-4.365329	12.733723
C	5.065684	1.171710	16.121876
H	4.473433	1.113777	17.038549
C	8.327233	-2.338088	10.115575
H	7.476721	-1.881763	9.605539
C	1.160183	-0.538382	12.802937
H	1.014814	-1.556877	13.170863
C	10.566577	-3.443145	11.373369
H	11.433512	-3.888553	11.867541
C	10.734109	-2.611650	10.263855
H	11.733648	-2.386341	9.883429
C	0.258241	1.524444	11.939292
H	-0.593001	2.126791	11.614699
C	9.611258	-2.071003	9.638253
H	9.722818	-1.423976	8.764249
C	0.061433	0.229275	12.414922
H	-0.946779	-0.188174	12.482490

Table S10 Optimized coordinates of **1** in CH₂Cl₂ with triplet spin state

Ru	5.351588	1.013822	10.160027
P	4.306418	1.926320	12.136994
S	4.327517	2.749927	8.866663
Cl	7.403312	2.168691	10.610830
Cl	6.344933	0.114057	8.179233
S	6.744255	-3.445338	12.073688
N	5.793694	-0.640945	11.112556
H	6.593008	-0.842100	11.715205
N	3.753747	-0.045207	9.684501
C	5.087582	1.451279	13.736054
C	5.085385	-1.706211	10.692791
C	3.963662	-1.401880	9.843146
C	5.036929	3.050015	7.252556
C	4.216323	3.752431	12.329514
C	2.587376	1.318834	12.266241
C	3.291170	-2.460186	9.215899
H	2.499521	-2.261672	8.496063
C	5.163228	4.565599	11.694531
H	5.907272	4.113736	11.034031
C	2.670169	0.546520	9.050506
C	4.595871	2.404953	6.097753
H	3.823408	1.635562	6.153898
C	4.314259	1.374187	14.904234
H	3.227907	1.480236	14.857887
C	2.813939	1.864147	8.547226
C	6.477819	1.308209	13.823989
H	7.092998	1.391887	12.923935
C	3.298512	4.330921	13.221421
H	2.563817	3.713349	13.742291
C	5.436033	-3.057131	10.946494
C	1.764109	2.524483	7.909053
H	1.919131	3.540104	7.536311
C	3.661706	-3.779363	9.470995
H	3.129395	-4.588117	8.966373
C	6.042385	4.018804	7.195834
H	6.389402	4.512647	8.106013
C	2.365041	0.008555	12.715707
H	3.202988	-0.613738	13.038722
C	5.188278	5.938337	11.946577
H	5.937087	6.563461	11.454640
C	8.252664	-3.153063	11.166349
C	1.499946	2.085907	11.831951
H	1.654189	3.096286	11.447513
C	1.395690	-0.046468	8.923161
H	1.200640	-1.015531	9.378584
C	0.359054	0.610752	8.273038
H	-0.612620	0.117086	8.192617
C	6.311336	1.033743	16.223715
H	6.792398	0.873047	17.191852

C	7.082160	1.098356	15.064330
H	8.168062	0.987094	15.121656
C	4.712737	-4.081751	10.345193
H	4.996528	-5.117974	10.542168
C	5.146550	2.763591	4.867797
H	4.789223	2.268099	3.961559
C	3.322317	5.703196	13.462783
H	2.602885	6.144310	14.157278
C	4.269527	6.507975	12.827171
H	4.297846	7.581675	13.031438
C	6.597371	4.355325	5.962314
H	7.381771	5.114821	5.913190
C	0.536425	1.891458	7.744212
H	-0.281553	2.402602	7.232880
C	6.141718	3.739646	4.795534
H	6.566444	4.025069	3.830007
C	9.414842	-3.677771	11.748477
H	9.344660	-4.280011	12.658491
C	4.924942	1.169051	16.140451
H	4.310548	1.116265	17.042558
C	8.339348	-2.401101	9.990995
H	7.452265	-1.983615	9.511019
C	1.071303	-0.503878	12.774157
H	0.907861	-1.518602	13.144610
C	10.657853	-3.421178	11.173053
H	11.556281	-3.834056	11.638759
C	10.753124	-2.646197	10.015109
H	11.727397	-2.431364	9.569105
C	0.205206	1.570103	11.897621
H	-0.635102	2.183885	11.566614
C	9.591061	-2.147546	9.427829
H	9.646352	-1.545254	8.517282
C	-0.012938	0.280560	12.378480
H	-1.027888	-0.120626	12.443718

Table S11 Optimized coordinates of $(T_R)_1^\bullet$ in CH_2Cl_2 with doublet spin state

C	-2.776323	1.029433	0.663606
C	-1.442206	0.645812	0.571386
C	-0.403899	1.609657	0.486629
C	-0.763148	2.975371	0.522367
C	-2.096158	3.351740	0.604190
C	-3.107333	2.385650	0.660872
H	-3.566825	0.279788	0.725333
H	0.026508	3.728996	0.461558
H	-2.358366	4.412940	0.617544
H	-4.155544	2.688113	0.716763
N	0.881286	1.180791	0.331857
H	1.566464	1.931943	0.259021
S	-0.810087	-1.012805	0.724460
C	-1.918578	-2.180537	-0.048011
C	-3.184663	-2.413951	0.501615
C	-1.421674	-3.003630	-1.059576
C	-3.971628	-3.443268	-0.013757
H	-3.545371	-1.820769	1.344548
C	-2.212263	-4.036792	-1.558441
H	-0.403931	-2.854995	-1.419143
C	-3.491437	-4.251498	-1.046177
H	-4.959310	-3.630781	0.414348
H	-1.817641	-4.678426	-2.350238
H	-4.110753	-5.061647	-1.438695
Ru	1.424079	-0.665167	0.085191
Cl	3.720746	0.034988	-0.091750
Cl	2.053705	-2.968897	-0.365496
P	1.839896	-1.069422	2.439694
P	1.311750	-0.252116	-2.358332
C	3.583413	-1.327545	2.959522
C	4.174925	-0.646580	4.029422
C	4.305775	-2.331985	2.298692
C	5.468987	-0.974891	4.440747
H	3.628341	0.135827	4.559888
C	5.590355	-2.663796	2.720214
H	3.850055	-2.850773	1.450864
C	6.175451	-1.987753	3.793688
H	5.921402	-0.436241	5.277250
H	6.142464	-3.451769	2.201535
H	7.179235	-2.259029	4.130854
C	1.035503	-2.510271	3.265977
C	1.189720	-2.682953	4.650461
C	0.328277	-3.474022	2.537796
C	0.629279	-3.786709	5.291482
H	1.755947	-1.953627	5.236290
C	-0.240197	-4.574225	3.183274
H	0.254380	-3.390446	1.452246
C	-0.097511	-4.729925	4.561255
H	0.768851	-3.915829	6.368082

H	-0.788458	-5.317073	2.597670
H	-0.540161	-5.591250	5.068356
C	1.259742	0.399689	3.364587
C	1.940051	1.613302	3.170536
C	0.086038	0.390308	4.125736
C	1.460813	2.787097	3.744507
H	2.842807	1.639022	2.552981
C	-0.393974	1.571188	4.697336
H	-0.465037	-0.539900	4.276485
C	0.291819	2.769286	4.510691
H	1.999475	3.724157	3.581397
H	-1.313270	1.549585	5.287600
H	-0.089185	3.691574	4.956604
C	2.625092	-1.067873	-3.357042
C	3.664918	-0.328047	-3.938089
C	2.611020	-2.459683	-3.541417
C	4.651141	-0.956281	-4.700172
H	3.711311	0.754104	-3.803030
C	3.585631	-3.082241	-4.321090
H	1.838350	-3.068192	-3.071990
C	4.610933	-2.335636	-4.902381
H	5.449108	-0.355909	-5.144289
H	3.541301	-4.163976	-4.473387
H	5.374898	-2.829466	-5.508684
C	1.486353	1.520941	-2.856093
C	0.737885	2.061406	-3.911280
C	2.447682	2.327058	-2.228903
C	0.947328	3.376396	-4.329050
H	-0.010200	1.453952	-4.423571
C	2.660816	3.637859	-2.654323
H	3.055672	1.906014	-1.423379
C	1.913680	4.166278	-3.706920
H	0.354341	3.780512	-5.153653
H	3.422207	4.247428	-2.161233
H	2.093330	5.188737	-4.049332
C	-0.269567	-0.700060	-3.192744
C	-0.386360	-1.591199	-4.265885
C	-1.432460	-0.100103	-2.687386
C	-1.642924	-1.902795	-4.790504
H	0.497617	-2.055059	-4.704851
C	-2.683552	-0.403481	-3.216488
H	-1.362644	0.613856	-1.863709
C	-2.793758	-1.321210	-4.262194
H	-1.718680	-2.607558	-5.622641
H	-3.574005	0.070912	-2.796441
H	-3.773414	-1.583103	-4.670244

Table S12 Optimized coordinates of $(T_R)_2^\bullet$ with doublet spin state

C	-1.117049	1.295739	0.340920
C	0.021182	0.639600	0.882069
C	0.809792	1.349693	1.806568
C	0.460975	2.640612	2.193821
C	-0.671767	3.256007	1.661377
C	-1.464082	2.582299	0.724479
H	1.697006	0.865569	2.221561
H	1.083055	3.172213	2.917532
H	-0.956054	4.261083	1.979299
H	-2.346775	3.063877	0.304314
N	0.242918	-0.645425	0.476215
H	1.057881	-1.108140	0.875483
O	-1.816186	0.540863	-0.560952
C	-2.948768	1.088483	-1.228225
H	-3.273939	0.308933	-1.928338
H	-3.740913	1.309008	-0.498031
H	-2.656634	1.995403	-1.778518
Ru	-0.938706	-1.444841	-0.823015
P	-2.468013	-2.425265	0.762132
Cl	-2.547349	-2.046630	-2.531882
Cl	0.274639	-3.481259	-0.696531
C	-1.702837	-2.937951	2.357982
C	-1.848443	-4.246648	2.836796
C	-0.885377	-2.051600	3.075192
C	-1.207222	-4.652268	4.005889
H	-2.459712	-4.964239	2.288278
C	-0.244989	-2.460661	4.242769
H	-0.726364	-1.035473	2.713007
C	-0.400212	-3.764358	4.711741
H	-1.342739	-5.675848	4.364160
H	0.386535	-1.753285	4.785557
H	0.108791	-4.087779	5.623005
C	-3.826783	-1.252352	1.182517
C	-4.940422	-1.195071	0.327430
C	-3.741124	-0.337851	2.240658
C	-5.956648	-0.267502	0.550694
H	-5.007372	-1.876937	-0.524375
C	-4.754853	0.597694	2.452899
H	-2.882483	-0.347458	2.915262
C	-5.868925	0.632259	1.614196
H	-6.823058	-0.249564	-0.115956
H	-4.671447	1.297455	3.288326
H	-6.668246	1.356641	1.792204
C	-3.379734	-3.935104	0.249891
C	-2.883936	-4.752355	-0.771047
C	-4.554278	-4.310016	0.920523
C	-3.560425	-5.919689	-1.122832
H	-1.960161	-4.473491	-1.277577
C	-5.223396	-5.480066	0.568726

H	-4.950156	-3.684969	1.724956
C	-4.730852	-6.282526	-0.461174
H	-3.164809	-6.548123	-1.924314
H	-6.135254	-5.764981	1.099101
H	-5.261053	-7.194186	-0.748190
P	0.436376	-0.722654	-2.652637
C	2.170389	-0.289157	-2.193224
C	2.862426	0.818442	-2.698717
C	2.830440	-1.155385	-1.308626
C	4.168898	1.084730	-2.288330
H	2.381709	1.491652	-3.411040
C	4.136180	-0.887141	-0.903027
H	2.310953	-2.048242	-0.945724
C	4.802871	0.242762	-1.377216
H	4.691572	1.957822	-2.686592
H	4.634549	-1.570121	-0.210073
H	5.817715	0.466161	-1.038328
C	0.682463	-1.812984	-4.111598
C	0.197135	-3.122777	-4.149235
C	1.372852	-1.302066	-5.221222
C	0.387838	-3.900625	-5.293093
H	-0.326694	-3.525299	-3.282745
C	1.560469	-2.081346	-6.358469
H	1.768837	-0.284059	-5.200366
C	1.059920	-3.383895	-6.398093
H	-0.004496	-4.919885	-5.317596
H	2.100634	-1.669660	-7.214711
H	1.202575	-3.998776	-7.290485
C	-0.256010	0.798776	-3.406642
C	-0.013532	2.063582	-2.851699
C	-1.141784	0.690835	-4.486894
C	-0.591299	3.202918	-3.409770
H	0.633784	2.167133	-1.977612
C	-1.732966	1.829466	-5.030817
H	-1.373316	-0.291944	-4.902833
C	-1.448214	3.089764	-4.505705
H	-0.363543	4.182044	-2.980084
H	-2.414149	1.726922	-5.879125
H	-1.898670	3.980622	-4.950293

References:

1. (a) G. M. Sheldrick, *Acta Crystallogr., Sect. C: Struct. Chem.*, 2015, **71**, 3-8; (b) G. M. Sheldrick, *Acta Cryst.*, 2008, **A64**, 112-122.
2. F. Neese, *Wiley Interdiscip. Rev.: Comput. Mol. Sci.*, 2012, **2**, 73-78.
3. (a) A. D. Becke, *J. Chem. Phys.*, 1993, **98**, 5648-5652; (b) B. Miehlich, A. Savin, H. Stoll and H. Preuss, *Chem. Phys. Lett.*, 1989, **157**, 200-206; (c) C. Lee, W. Yang and R. G. Parr, *Phys. Rev. B*, 1988, **37**, 785-789.
4. (a) F. Weigend and R. Ahlrichs, *Phys. Chem. Chem. Phys.*, 2005, **7**, 3297-3305; (b) F. Weigend, F. Furche, and R. Ahlrichs, *J. Chem. Phys.*, 2003, **119**, 12753-12762; (c) K. Eichkorn, F. Weigend, O. Treutler and R. Ahlrichs, *Theor. Chem. Acc.*, 1997, **97**, 119-124; (d) A. Schaefer, C. Huber and R. Ahlrichs, *J. Chem. Phys.*, 1994, **100**, 5829-5835; (e) A. Schaefer, H. Horn and R. Ahlrichs, *J. Chem. Phys.*, 1992, **97**, 2571-2577.
5. (a) S. Kossmann and F. Neese, *J. Chem. Theory Comput.*, 2010, **6**, 2325-2338; (b) H. B. Schlegel and J. J. McDouall, *In Computational Advances in Organic Chemistry*. C. Ogretir, I. G. Csizmadia, Eds.; Kluwer Academic: The Netherlands, 1991.
6. (a) R. E. Stratmann, G. E. Scuseria and H. Frisch, *J. Chem. Phys.*, 1998, **109**, 8218-8224; (b) M. E. Casida, C. Jamoroski, K. C. Casida and D. R. Salahub, *J. Chem. Phys.*, 1998, **108**, 4439-4449; (c) R. Bauernschmitt, M. Haser, O. Treutler and R. Ahlrichs, *Chem. Phys. Lett.*, 1996, **256**, 454-464; (d) M. Cossi, N. Rega, G. Scalmani and V. Barone, *J. Comput. Chem.*, 2003, **24**, 669-681; (e) V. Barone and M. Cossi, *J. Phys. Chem. A*, 1998, **102**, 1995-2001.
7. (a) A. D. Becke, *J. Chem. Phys.*, 1993, **98**, 5648-5652; (b) B. Miehlich, A. Savin, H. Stoll and H. Preuss, *Chem. Phys. Lett.*, 1989, **157**, 200-206; (c) C. Lee, W. Yang and R. G. Parr, *Phys. Rev. B*, 1988, **37**, 785-789.